A SIMPLIFIED WOOD COMBUSTION MODEL
FOR USE IN THE SIMULATION OF COOKING FIRES.

Burnham-Slipper H*, Clifford MJ and Pickering SJ.
*Author for correspondence
Department of Mechanical, Materials and Manufacturing Engineering,
University of Nottingham, NG7 2RD, England
E-mail: eaxhb@nottingham.ac.uk

ABSTRACT

Wood combustion was studied with the intention of developing a simplified model of fuel burn-rate in small cooking fires, for inclusion in a CFD model of a whole cook-stove. The investigation included collecting experimental data on fuel burn-rate, model development and comparison of experimental and simulation results. In the experimental phase, regular blocks of wood were arranged in a lattice or crib with a range of volumes, void fractions and specific surface areas. The burning cribs yielded 3-40 kW fires. The simplified model assumed an unreacted core of virgin wood surrounded by char. It included considerations of heat transfer through the fuel by conduction; thermal decomposition of the virgin fuel into char and volatile gases, limited by the supply of heat to the pyrolysis region; the surface combustion of char limited by the diffusion of oxygen through the species boundary layer and impeded by the counter-flow of volatile gases. The model predicted the change of burn-rate with crib volume, porosity and surface area shown by experimental data, though it does incur significant errors, due to the assumption of one-dimensional behaviour within the crib, and neglecting spatial and temporal variations in boundary conditions. It was concluded that accuracy of the model could be improved by developing it to two or three dimensions, and that the easiest way to do this was through CFD. The model was sufficiently accurate to be used as a source of wood volatiles when modelling small fires in cook-stoves, with the aim of investigating the effect of design changes on stove efficiency.

NOMENCLATURE

a	[-]	normalised crib specific area
A	[m^{-1}]	specific area
A	[m^2]	area
b	[-]	blowing parameter
c	[J/kgK]	specific heat capacity
c_{f0}	[-]	dimensionless group
D	[m]	diameter
G	[kg/m^{2}s]	mass flux
Gr	[-]	Grashof number
h	[m]	block dimension - height
h	[J/kg]	specific enthalpy
h_h	[W/m^{2}K]	convective heat transfer coefficient
h_m	[m/s]	convective mass transfer coefficient
k	[W/mK]	thermal conductivity
l	[m]	block dimension - length
Le	[-]	Lewis number
M	[kg/m^3/s]	specify burn-rate
n	[-]	number of blocks per layer
Nu	[-]	Nusselt number
p	[-]	normalised crib porosity
P	[-]	porosity
Pr	[-]	Prandtl number
Q	[W]	heat
Re	[-]	Reynolds number
S	[K/s]	temperature source
T	[K]	temperature
t	[s]	time
U	[m/s]	velocity
v	[-]	normalised crib volume
V	[m^3]	volume
w	[m]	block dimension - width
ε	[-]	emissivity
ρ	[kg/m3]	density
σ	[W/m^{2}K^4]	Stefan-Boltzmann constant
σ	[-]	sensitivity

Subscripts

∞	free-stream
$char$	char
$evap$	evaporation
$o2$	oxygen
$pyro$	pyrolysis
s	surface
v	volatiles

INTRODUCTION

Wood, agricultural residues and other biomass fuels typically burn through a multi-stage process of thermal decomposition, flaming combustion and char oxidation. It is a process which is of key importance to many millions of families in low-income countries who cook on wood-burning stoves and open fires. Though fuel is often free at the point of use, there are hidden costs associated with time spent collecting wood and time lost through ill-health due to pulmonary and peri-natal complications associated with indoor air pollution. The work

reported here is the first part of a project to improve wood-burning stoves: we aim to develop a model of fuel burn-rate in small wood fires. It is not intended as a general model, but is developed with the specific intent of predicting the rate of release of volatile matter in a larger CFD model of a complete cooking stove. We are particularly interested in the quasi-steady period of the fire, after flames have taken hold of all the fuel surfaces, but before it dies down to a pile of smouldering charcoal, since an experienced operator will maintain a cooking fire in this condition: other fire conditions are beyond the scope of this investigation.

Previous investigators have examined conditions inside pieces of charring fuel by developing energy and heat balances to record the progress of the evaporation and pyrolysis fronts through the fuel. Di Blasi's model [1] is possibly the most complete and demonstrated that gas and solid are in thermal equilibrium, a thin pyrolysis front progresses through the fuel particle, and that convection of volatile gases to the char surface is effectively instantaneous. Saastamoinen & Richard [2] demonstrated that heat transfer (not kinetics) limits the rate of pyrolysis for large particles. Bellais et al. [3] investigated a variety of models for the shrinkage of char, concluding that the effect of shrinkage can be ignored given the uncertainty in other parameters. Bryden et al. [4] identified several different pyrolysis regimes (as a function of heating rate and fuel thickness), of which the slowest is a pyrolysis wave: the drying and pyrolysis regions are close and thin for much of the burn-out time. This supports the simplification to a single decomposition wave containing both drying and pyrolysis.

Surface char combustion is a source of heat and gas species, and significantly affects the supply of heat to the unreacted fuel. Consequently it must be included in a full account of biomass combustion. Fredlund [5] modelled a kinetically limited char reaction, in which char burns incompletely with oxygen at the fuel surface to yield carbon monoxide. Boonmee & Quintiere [6] demonstrated that above a certain temperature (~700K) char combustion is limited by the diffusion of oxygen to the char surface. Ouedraogo et al. [7] identified that blowing volatile gasses through the char surface tends to inhibit the transfer of heat and mass from the free-stream to the fuel.

An account of a whole fuel bed was given by Brunch et al. [8], who developed a one-dimensional model of a fuel particle, then populated a fixed bed with a finite number of particles in a transient CFD simulation of a wood fire. Their model requires that the mass and position of each particle be tracked as the bed collapses, leading to a very expensive calculation.

The aim of this study was to develop a robust yet computationally cheap model of volatile evolution and char combustion in fixed bed conditions, which can subsequently be included in a CFD code to give an instantaneous account of a well tended wood fire. The boundary conditions that the model can access from the CFD code are gas temperature, velocity and oxygen concentration. The paper contains a description of an experimental investigation of burning small wood cribs, a simplified model of wood combustion, and an assessment of the model's performance with respect to experimental data.

EXPERIMENTAL SET-UP

Cribs were built of pine blocks. The blocks were knot free, with the grain running the length of the block. Fuel properties (table 1) were found using the procedure defined in BS1016 (for the proximate analysis for coal).

Table 1. Fuel properties

Parameter	Value
Virgin fuel density	450 ± 10 kg/m^3
Moisture fraction	9.5 ± 0.6 %
Volatile fraction	74.6 ± 0.4 %
Virgin fuel gross calorific value	17.6 ± 0.2 MJ/kg
Char calorific value	29.8 ± 0.6 MJ/kg

Crib dimensions are defined in figure 1. All cribs were cubes, having l/h layers. Crib dimensions and properties are given in table 2. The dimensions of cribs A to I were selected as a factorial experiment in factors volume, void fraction and specific area (fuel surface area per unit crib volume), in order to assess the impact of fuel bed structure on burn-rate.

*Table 2.* Fuel block dimensions and resulting crib properties.

Crib	Dimensions [mm]				Volume	Void fraction	Specific Area
	l	h	w	n	[m^3]	[#]	[m^2/m^3]
A	160	20	5	13	0.004	0.6	192
B	160	20	20	3	0.004	0.6	66
C	160	20	10	13	0.004	0.2	188
D	160	20	30	4	0.004	0.3	78
E	140	20	12	7	0.0027	0.4	133
F	100	20	5	8	0.001	0.6	192
G	100	20	20	2	0.001	0.6	72
H	100	20	10	8	0.001	0.2	192
I	100	20	40	2	0.001	0.2	72
J	100	20	20	3	0.001	0.4	60
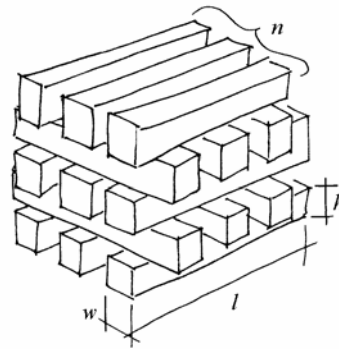
Figure 1. Dimensions for wood blocks for cribs: block length (l), height (h) and width (w), and the number of blocks per layer (n).

The crib was positioned on a flat plate on a balance (Mettler Toledo 32000). Four K-type thermocouples (0.75 mm bead diameter) were suspended in the crib (figure 2), measuring the gas temperature. These thermocouples give boundary conditions for the current model, though they play a more

significant role in validating the subsequent CFD model. An extraction hood with mean inlet velocity of *0.13* m/s was suspended *0.7* m above the base of the crib. A *3-4* g charge of firelighter was inserted into the bottom centre of the crib and lit, after which mass and temperature data were logged at *0.1* Hz, until burn-out.
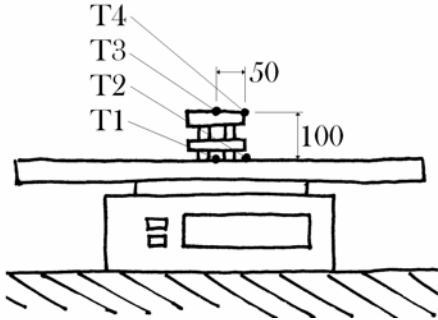
Figure 2. *Wood-crib on the balance, with the locations of the thermocouples (T1 to T4). Dimensions in mm.*

MODEL DEVELOPMENT

In developing the model it was assumed that:

- the crib was built of sticks with circular cross-section (dimensions of the rectangular blocks given in table 2 were modified to give an effective radius using a mass-conservation criterion);
- all the blocks in the crib burned at the same rate, and end effects were ignored;
- all fuel surfaces were subject to the same boundary conditions, corresponding to mean temperature, velocity and oxygen concentration within the crib.

The problem was thus simplified to one-dimension (i.e. radial position, *r*, in the fuel block). This section describes heat transfer, thermal decomposition and char combustion, as well as boundary and initial conditions used in the model.

Heat transfer

Distribution of temperature, T, within the fuel was given by:

$$\frac{\partial T}{\partial t} = \frac{k(T)}{\rho(T)c(T)}\frac{\partial^2 T}{\partial r^2} + S \tag{1}$$

Thermal conductivity *k(T)* and specific heat capacity *c(T)* are defined in table 3. Fuel density, *ρ(T)*, is discussed below.

Thermal decomposition

Thermal decomposition of wood included driving off moisture at *373* K, and driving off volatile gases over a wider temperatures range (typically *473-573* K).

It was assumed that evaporation of moisture was kinetically quick and that the evolved gas dispersed immediately. The fuel was allowed to heat up until the temperature exceeded the evaporation temperature. If the density of the element was found to be greater than that of dry fuel (i.e. it still contained moisture) then the temperature was capped to the evaporation temperature, and the sensible heat associated with this excess

temperature was used to reduce the density (i.e. drive off moisture):

$$\text{if } T > T_{evap} \text{ and } \rho > \rho_{dry} \text{ then } \Delta\rho = -\frac{(T - T_{evap})\rho c}{h_{evap}}$$

$$\text{and } T = T_{evap} \tag{2}$$

The same method was applied to the devolatalisation process, except the temperature and enthalpy of evaporation (T_{evap} and h_{evap} in equation (2)) were replaced by the temperature and enthalpy of pyrolysis, T_{pyro} and h_{pyro}. Though the pyrolysis process is slower than the evaporation of moisture and occurs over a wider temperature range, the work of Bryden et al. [4] demonstrated that the assumption of a thin pyrolysis wave was adequate.

Boundary condition

The surface of the fuel received energy from convection, radiation and char combustion:

$$Q_s = h_h A_s (T_c - T_s) + \sigma A_s \varepsilon (T_c^4 - T_s^4) + Q_{char} \tag{3}$$

where T_c is the crib temperature (boundary condition, taken from experimental data). In a separate study, embers were photographed as they rose from the crib. From the length of the traces, the velocity of gas leaving the crib was estimated as 1 ± 0.15 m/s. Using this velocity and the mean space between blocks as characteristic length, the Reynolds number of the flow inside the crib was estimated as 50<Re<500. Hence laminar conditions were assumed, and convection heat transfer coefficient, h_h, was given by an experimental correlation for laminar natural convection flow over a cylinder (Jaluria, 2003):

$$\overline{Nu} = \frac{h_h D}{k} = 0.436(Gr\,\text{Pr})^{0.25} \tag{4}$$

where *D* is the fuel diameter, *Gr* is the Grashof number and *Pr* is the Prandtl number. Grashof number was calculated from fuel diameter and difference in temperature between char surface and ambient air (300K). The Nusselt number was corrected to account for the transpiration of volatile gases through the char layer, which tended to inhibit the interaction of the surface with the free-stream flow, using the correlation [10]:

$$\frac{\overline{Nu}_b}{\overline{Nu}} = \frac{b}{e^b - 1} \tag{5}$$

where b is the blowing coefficient, defined as:

$$b = \frac{G_v / G_\infty}{c_{f0}} \tag{6}$$

G_v is the surface mass flux of volatile gases and G_∞ is the free-stream mass flux. c_{f0} is the dimensionless group:

$$c_{f0} = \frac{\tau_0}{\rho_\infty u_\infty^2} \tag{7}$$

Boundary shear stress, τ_0, was evaluated from Blasius (see [11]):

$$\tau_0 = 0.365 \frac{\rho_\infty u_\infty^2}{\sqrt{Re}} \tag{8}$$

Char combustion

Once the surface of the fuel had pyrolised, it burned with oxygen to give carbon monoxide. The reaction was limited by the diffusion of oxygen through the species boundary layer. The rate of char consumption was given by [7]:

$$\frac{d\rho_s}{dt} = \frac{12}{16} \frac{A_s}{V_s} \rho_{O2\infty} h_m \tag{9}$$

where A_s and V_s are the surface area and volume of the surface element, and h_m is the mass transfer coefficient, given by a correlation to the heat transfer coefficient [12]:

$$\frac{h_h}{h_m} = \rho c_p Le^{0.5} \tag{10}$$

The Lewis number, Le, was taken to be 1.35 for air at 900K. The char combustion heat source in equation (2) can now be given as:

$$Q_{char} = \frac{d\rho_s}{dt} V_s h_{char} \tag{11}$$

RESULTS

Experimental Results

Typical experimental data is presented in figure 2, showing temperatures at 4 locations in the crib and the non-dimensional crib mass (m/m_0, ratio of crib mass to initial crib mass). After ignition the temperature near the centre-line rose quickly to *600* K and rose steadily thereafter. Crib mass fell very slowly at first, gradually increasing as temperature increased and flames spread through the crib.
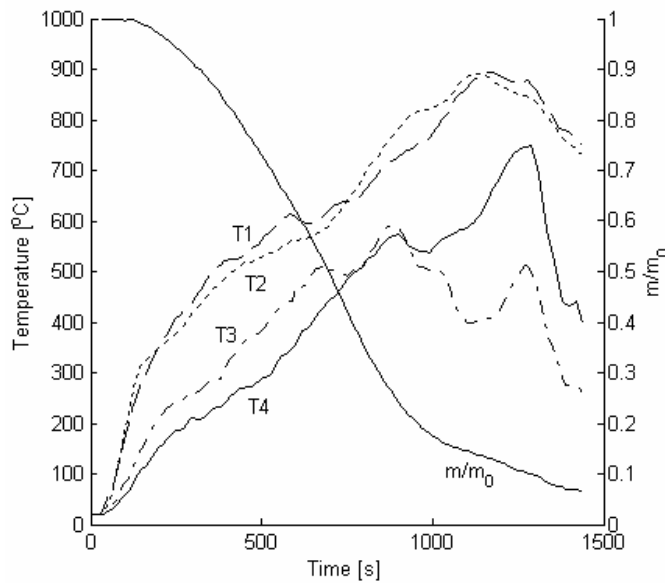
Figure 3. Typical experimental results for crib combustion (Crib J). Temperatures T1 to T4 defined in figure 2.

Once fire had taken hold of all the fuel surfaces (*~500* s), mass fell at a steady rate until all the volatile matter had been driven off (*~1000* s). Subsequent mass loss was due to char combustion alone. The mean fuel consumption rate and crib temperatures were taken for each crib during the quasi-steady period in the range *0.8>m/m_0>0.2* and used for comparison with the simulation results. During this period the effect of initial ignition conditions was no longer significant, nor was the fire dominated by smouldering char combustion.

Cribs C and H smouldered throughout the tests, and did not produce a flame despite several re-runs. It was concluded that the wood was cut too fine and packed too tight for adequate mixing between oxygen and volatile gases. Data from all cribs A to I were reduced using analysis of variance [17] to give specific burn-rate, *M*:

$$M = 0.33 + 0.00v + 0.11p + 0.06a \pm 0.08 kg/m^3.s \tag{12}$$

where *v*, *p* and *a* are normalized crib volume, porosity and density. Similarly, mean crib temperature was given by:

$$T = 900 + 0v + 100p - 100a \pm 100K \tag{13}$$

It is clear from (12) and (13) that specific burn-rate and crib temperature are independent of crib volume in this study, however cribs with a higher porosity and higher surface area tend to burn faster since oxidant could enter the crib and mix with volatile gases more easily.

Simulation results

The equations (1) to (11) were discretised using the finite difference method, to give a series of concentric radial elements (figure 4). The resulting set of simultaneous differential equations was solved with time steps of *0.05* s, using the Euler method. Fuel properties are given in table 3. For boundary conditions, the temperature was taken from mean experimental crib temperature, velocity was assumed to be 1 m/s and oxygen mass fraction was assumed to be *0.23*. All fuel elements were initially at *300* K.
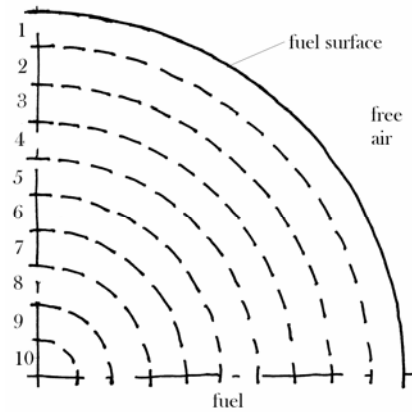
Figure 4. Fuel discretised into ten concentric elements, with element 1 initially acting as the fuel surface.
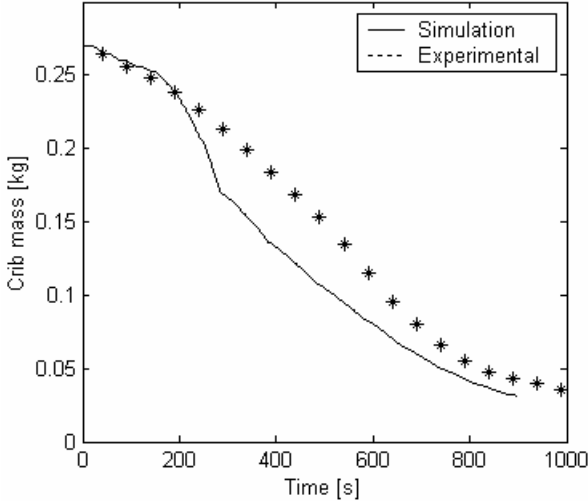
Figure 5. Crib mass from experimental and simulated data (Crib J).

Simulations were run of the cribs described in table 2, except C and H. Mass data is shown for crib J in figure 5, while the evolution of density and temperature in some of the elements in the simulation of crib J are shown in figures 6 and 7.

From figure 5 it is clear that the model predicts the initial acceleration of burn-rate, and predicts the steady loss of mass over the majority of the combustion time.

From figure 6 it is clear that the outermost region of the fuel (element 1) heats up quickly, with plateaus at *373* K (*20 – 50* s) while moisture is driven off and 550K (*140 – 240* s) when the fuel pyrolises. Subsequent discontinuities in temperature of element 1 are the result of other elements reaching the end of the pyrolysis period, and suddenly changing temperature. The use of a finer grid mitigates this behaviour. The use of an Arrhenius-style reaction rate for pyrolysis would eliminate this behaviour altogether, as pyrolysis would take place over a wide temperature range as a smooth, continuous process. Further away from the fuel surface, the temperature rate is slower, until in the innermost element, temperature rises to evaporation temperature as a smooth second-order response, and rises to the pyrolysis temperature as a smooth first order response.

From figure 7 it is clear that the wave of fuel decomposition travels through the fuel. There is a sharp change in density for element 1 from *20* to *50* s during moisture evaporation, corresponding to the temperature plateau in figure 6, and another corresponding to the pyrolysis period. After *240* s, the rate of decomposition of element 1 drops significantly, as the char begins to burn slowly. Once the char of element 1 has burned out (~*600* s), the char of element 2 starts to burn.

A sensitivity study was carried out, and reported in table 3. For each parameter used in the model, the nominal value and its source are given in columns 2 and 3. The sensitivity, σ, in column 4 measures the impact of any parameter on the fuel burn rate, defined as:

$$\sigma = \frac{\Delta M / M_0}{\Delta \Phi / \Phi_0} \tag{14}$$

where $\Delta M/M_0$ is the percentage change of burn-rate, and $\Delta \Phi/\Phi_0$ is the percentage change of the parameter. It is clear that the model is most sensitive to changes in fuel volatile fraction, devolatalisation temperature, crib temperature (which is a boundary condition) and char thermal conductivity. It is therefore important to identify accurate values of these parameters in order to produce an accurate model of crib combustion.
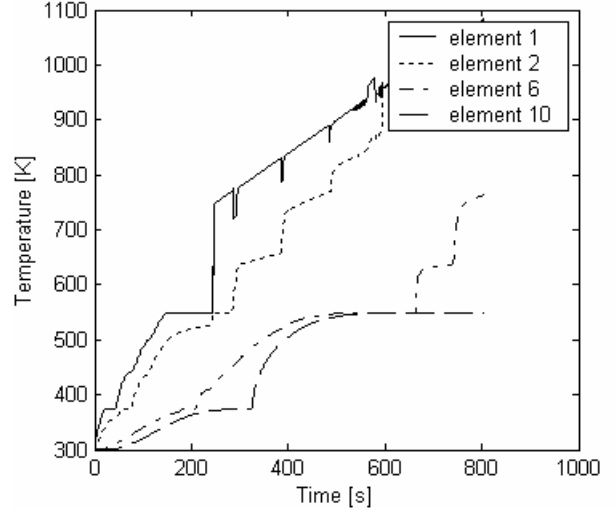

Figure 6. Temperature profile within the fuel (Crib J).
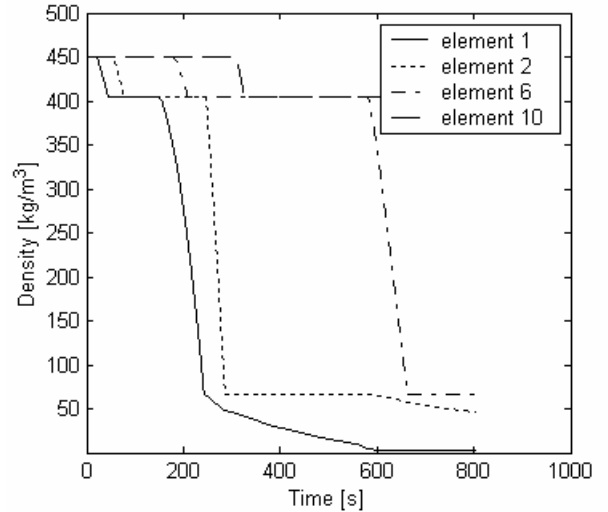
Figure 7. Density profile within the fuel (Crib J).

The fuel consumption rates from the theoretical model can be compared with experimental results, as in figure 8. The theoretical model gave a reasonable account of crib burn-rates: most results are within the ±30% limits though the greatest error is 48%. These errors were probably due to (a) inaccuracies in the surface area to volume ratio of fuel in the model due to the need to convert from rectangular cross-section to circular cross-section, and neglecting the block ends; (b) large variations in crib temperature in the experimental data; (c) the use of uniform boundary conditions, such that no account is made of whether a piece of fuel lies near the centre or near the edge of the crib. The accuracy of the model could be improved

by extending it to two or three dimensions, thereby taking into account the variation of boundary conditions within the crib. This is a task that lends itself to the use of CFD, where spatial discretisation in two or three dimensions has already been affected.

Table 3. Parameter values and sensitivity for the numerical model.

Parameter	Value	Source	Sensitivity
Virgin fuel:			
specific heat	150+5.8T J/kgK	[13]	-0.07
therm. cond.	0.055+0.0002T W/mK	[13]	0.07
density	450 kg/m^3	BS 1016	0.00
moisture frac.	0.1	BS 1016	-0.13
volatile frac.	0.75	BS 1016	2.10
Dry fuel:			
specific heat	100+3.9T J/kgK	[13]	-0.18
therm. cond.	0.035+0.0002T W/mK	[13]	0.31
Pyrolysis:			
temperature	550 K	[14]	-1.51
enthalpy	1.5 MJ/kg	[15]	-0.45
Char:			
specific heat	1390+0.36T J/kgK	[13]	-0.05
therm. cond.	0.07 W/mK	[16]	0.58
calorific value	30.0 MJ/kg	BS 1016	0.04
emissivity	0.8	[13]	-0.02
Crib temperature	variable	---	1.15
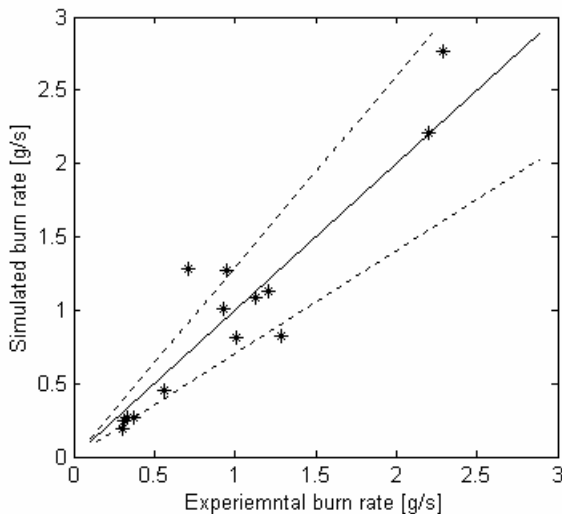
Figure 8. Comparison of simulated and experimental burn-rate during the period 0.2<m/m$_0$<0.8. The solid line is 1:1 and the dashed lines represent ±30% error.

In both experimental and modelling investigations, the blowing of volatiles inhibited oxygen from reaching the char until almost all the fuel had pyrolised, leaving a stack of unburned char. It also demonstrates that for the fires under investigation here, it is sufficient to model the pyrolysis and char combustion stages separately, as they are unable to occur in the same region of the fuel bed simultaneously.

SUMMARY & RECOMMENDATIONS

An experimental investigation into wood-crib combustion has been carried out to assess the burn-rate of small wood cribs, resulting in an experimental correlation of mass loss as a function or crib volume, porosity and surface area. A simplified model of crib combustion was developed, including heat transfer within the fuel, thermal decomposition, char combustion, and the effect of volatile transpiration on oxygen diffusion to the fuel surface. By comparing simulation and experimental data, it can be shown that the model exhibits significant errors due to the assumption of one-dimensional behaviour and uniform temperature and velocity conditions within the crib, however it has identified the trend of higher mass loss rate with increased crib volume, porosity and surface area. Further accuracy could be gained by extending the model to two or three dimensions. The model is a first step in gaining a full understanding of wood combustion, and is sufficiently accurate to predict the rate of volatile gas release from a burning wood crib in a CFD model of a complete stove, with the ultimate aim of assessing the impact of design changes on stove efficiency.

REFERENCES

[1] DiBlasi C, 1993. Modelling and simulation of combustion processes of charring and non-charring solid fuels. Prog. Energy Combust. Sci. 19:71-104.
[2] Saastamoinen J & Richard JR, 1996. Simultaneous drying and pyrolysis of solid fuel particles. Combust. Flame 106:288-300.
[3] Bellais M et al., 2003. Pyrolysis of large wod particles: a study of shrinkage importance in simulations. Fuel 82:1541-1548.
[4] Bryden et al., 2002. Modelling thermally thick pyrolysis of wood. Biomass and Bioenergy 22:41-53.
[5] Fredlund B, 1993. Modelling of heat and mass transfer in wood structures during fire. Fire Safety Journal 20:39-69.
[6] Boonmee N & Quintiere JG, 2005. Glowing ignition of wood: the onset of surface combustion. Proc Combustion Inst. 30:2303-2310.
[7] Ouedraogo et al., 1998. Quasi-steady shrinking core analysis of wood combustion. Combustion & Flame 114:1-12.
[8] Brunch et al., 2003. Modelling wood combustion under fixed bed conditions. Fuel 82:729-738.
[9] Jaluria, 2003. Natural convection, in Heat Transfer Handbook, Bejan A & Krauss AD (eds), John Wiley, New York, 2003.
[10] Kays WM & Crawford ME, 1993. Convective heat and mass transfer, 3rd ed. McGraw-Hill, New York.
[11] Massey BS, 1968. Mechanics of fluids. Chapman & Hall, London.
[12] Majumdar, 2005. Computational methods for heat and mass transfer. Taylor & Francis, New York.
[13] Ragland et al., 1991. Properties of wood for combustion analysis. Bioresource Tech. 37:161-168.
[14] Larfeldt J et al., 2000. Modelling and measurement of heat transfer in charcoal from pyrolysis of large wood particles. Biomass & Bioenergy 18:507-514.
[15] Demirbas, 2004. Combustion characteristics of different biomass fuels. Prog. Energy Combust. Sci. 30:219-230.
[16] Daugaard DE & Brown RD, 2003. Enthalpy for pyrolysis of several types of biomass. Energy & Fuels 17:934-939.
[17] Montgomery DC, 2005. Design and analysis of experiments. Wiley & Sons, Hoboken, NJ.